OPTIMIZATION OF BIOTECHNOLOGICAL PROCESSES. THE ACETIC ACID FERMENTATION. PART II: PRACTICAL IDENTIFIABILITY ANALYSIS AND PARAMETER ESTIMATION

Jorge E. Jiménez-Hornero,[(a)*] Inés M. Santos-Dueñas,[(b)] Isidoro García-García[(b)]

[(a)] Computing and Numerical Analysis Department, University of Cordoba, Spain

[(b)] Chemical Engineering Department, University of Cordoba, Spain

Abstract

In part I of this series a mathematical model for acetic acid fermentation was reported. However, no kinetic model can be complete until its equation parameters are estimated. This inevitably entails a practical identifiability analysis intended to ascertain whether the parameters can be estimated in an unambiguous manner based not only on the sensitivity of the model to them, but also on the amount and quality of available experimental data for this purpose. Also, estimating the model parameters entails optimizing a specific objective function subject to the model equations as major constraints and to additional, minor constraints on variables and parameters. This approach usually leads to the formulation of a non-linear programming problem involving differential and algebraic constraints where the decision variables constitute the parameter set to be estimated. In the scope of modelling biotechnological processes, this problem uses not be properly dealt with. This second paper reviews available models for practical identifiability assessment and parameter estimation with a view to their prospective application to the proposed model and its validation.

*Corresponding Author. Tel: +34 957212079; fax: +34 957218630
Address: Edif. Leonardo Da Vinci.
Campus Universitario de Rabanales.
Ctra. Madrid (a) Km. 396.
Postal Code: 14071 – Cordoba (Spain).
Email: jjimenez@uco.es

Keywords: Bioreactor systems; Kinetics; Modelling; Optimization; Acetification; Vinegar.

1. Introduction

1.1. Practical identifiability

Calibration or parameter estimation is one of the most critical steps in developing a grey-box model [1]. The procedure involves using experimental data for the target process the amount and quality of which strongly influence the quality of the resulting estimations [2]. Also, the model concerned may be poorly sensitive to changes in parameter values and considerably hinder their precise estimation as a result. Practical identifiability procedures are used to examine whether specific model parameters can be accurately determined with provision for all these factors [3].

1.1.1. The Fisher Information Matrix (FIM)

The core of a practical identifiability study is the Fisher Information Matrix (FIM) [4–6]. This is constructed from a weighted least-squares (WLS) objective function which is in turn obtained from the maximum likelihood estimator as determined under the assumption of normally distributed measurement noise of zero mean. The procedure typically used to construct the FIM is described in detail elsewhere [7–10]. This matrix, of $p \times p$ dimensions (p being the number of model parameters), essentially provides a compact representation of measurement uncertainty and the parameter sensitivity of the model.

The sensitivity functions, included in the FIM, constitute the core of the sensitivity analysis [8,11–18], which is usually of local nature for biological processes by virtue of the models typically applied to them using non-linear parameters. A graphical sensitivity analysis allows one to identify the individual parameters most strongly

influencing the dynamics of the target system [11,19,20]. The greater a function is, the higher will be the sensitivity of the chosen output to changes in the function parameter concerned and the greater the information content of the output towards the identification of the parameter. Otherwise, the output will be poorly sensitive to the parameter and of little use for its estimation. When the graphs for two or more parameters are similarly shaped, one can expect output variations caused by a change in some parameter under the experimental conditions used to be virtually offset by a change in one or more of the others, and assume the parameters to be correlated [2,8,10].

Sensitivity functions can be calculated with various procedures [10,22] including the finite difference approximation (also known as the "indirect method"), the direct method [28], the Green function method [29] (also referred to as the "variation method"), the polynomial approximation method [30,31], automatic differentiation techniques [32,33] and the complex-step derivative approximation method [34]. Some of these algorithms have the disadvantage that they require introducing some heuristics in their application or that the user must fix some parameters in order to adjust their behaviour. This alters convergence and precision in the output. Given the highly sophisticated computations afforded by available numerical integrators such as LSODE [35] and DASSL [36], the direct method constitutes the most easily implemented choice for state–space models and provides acceptably precise calculations at a low computational cost. In fact, the direct method requires no heuristics and its performance is uninfluenced by parameters other than those associated to the numerical integrators used.

The FIM can be calculated at any point in time, but is usually computed throughout an experiment (homoscedastic measurement errors), whether because a simplified starting

hypothesis is adopted or because the instrumental measurements are all subject to a roughly constant error. Because starting hypotheses frequently assume output measurements to be independent, these elements will invariably be zero.

1.1.2. Methods for evaluating practical identifiability

Practical identifiability can be preliminarily assessed by calculating the FIM rank. If the rank is smaller than *p*, then the model will be practically unidentifiable and one or more FIM eigenvalues will be zero. However, one may have a full-rank FIM and the model parameters still be hard to identify. This has led some authors [8,10] to propose the use of the FIM condition number in order to assess whether model parameters will be practically identifiable. This criterion, however, has the disadvantage that it is parameter unit-dependent; because no reference critical value is available for comparison and discrimination [21,22], the results are not always accurate. Alternatively, one can use the so-called "collinearity index" [23], η_m, instead of the condition number; as conceded by its proponent, however, the two quantities result in only slight differences. There are additional criteria which are typically used as objective functions in optimal experimental design for parameter estimation [2,6,10,14,24–27]. The indices involved are used to assess parameter sensitivity or correlation, but cannot by themselves solve the problem of practical identifiability —in fact, the above-mentioned condition number constitutes one such criterion: the so-called "modified E-optimal criterion". The most effective alternative with a view to the assessment of practical identifiability in a model is to calculate the correlation matrix for the estimated parameters, which can expose linear dependences between them. In summary, the most suitable procedure for assessing local practical identifiability should involve the direct, joint analysis of the sensitivity functions and that of the parameter estimation correlation matrix.

The correlation matrix arises from the parameter estimation error covariance matrix [37], which involves the calculation of the hessian matrix of the objective function with respect to the parameter values obtained at the optimum. There are several numerical choices for calculating this Hessian matrix: a quadratic approximation to the objective function around the optimum [38,39], Taylor series expansion, Richardson's extrapolation as such [40] or combined with the complex-step derivative approximation technique [34,41], the method of Marsili-Libelli *et al.* [42] or *quasi*-Newton optimization algorithms [43]. However, the method based on the FIM approximation is the most widely used by far for this purpose [10,40,42]. The goodness of its results increases with increasing accuracy of the model and decreasing distance to the optimum; under such conditions, the hessian is, approximately, two times the FIM [22].

Parameter estimation error covariance matrix is the core of the asymptotic parameter confidence region at the optimum [2,8,10,22], which can be used to calculate the confidence interval for each parameter [22,44–48]. Also, this matrix can be used to determine the elements of the parameter estimation correlation matrix which, as noted earlier, when combined with sensitivity functions, is the essential tool for practical identifiability analysis.

1.1.3. Determining the subset of most identifiable parameters

Based on the foregoing, the typically high complexity of biotechnological process models frequently makes them practically unidentifiable. In any case, it is still interesting to identify the subset of parameters that can be unambiguously determined by using an appropriate optimization algorithm. This is important since, even though the results would largely lack physical meaning, they would still allow the model to be highly accurately calibrated from experimental data. The most widely used methods for determining the subset of identifiable parameters include the following [22]: model

reduction, Monte Carlo techniques [49–52], regression methods [53], visual inspection of local sensitivity functions [16,23,54–58], Principal Component Analysis (PCA) [59], methods based on specific FIM characteristics [14–16,55], parameter selection methods based on the collinearity index [23] and an improved method based on FIM characteristics [22]. The last procedure, which was adopted in this work, relies on the relationship between the Hessian of the objective function and FIM in order to calculate the parameter estimation correlation matrix, which is subsequently used to identify the most practically identifiable individual parameters. As shown later on, this technique was combined with parameter estimation methodology.

1.2. Parameter estimation

Estimating the parameters of a model entails optimizing an objective function dependent on a norm for the error made in measuring the process outputs [60]. The specific norm to be used depends on the statistical distribution of the measurement errors [61]. If the errors are normally distributed, have a zero mean and a known covariance matrix, then one can use the following weighted least-squares function, which constitutes a maximum likelihood estimator [10].

The minimization of this objective function is addressed as a non-linear programming (NLP) problem largely subject to the constraints imposed by the model equations — which are also typically non-linear. Given the specific nature of the problem, the objective function is frequently multi-modal (non-convex), which makes identifying the overall minimum rather a difficult task [60].

1.2.1. Overview of optimization methods

As a rule, the optimization problem has no trivial solution. This has fostered the development of a number of techniques of the local or global type. The latter are

especially attractive for the problem at hand as they aim to find the global optimum of the objective function —which usually exhibits many local optima.

Optimization tools for this purpose can also be classified as deterministic (both local and global) and stochastic (largely global). The former aim to verify the necessary and sufficient optimality conditions by calculating search directions in a systematic manner. If the problem at hand is subject to no constraints, then the optimality conditions are $\nabla J\left(v^*\right)=0$ and $\nabla^2 J\left(v^*\right)>0$, v^* being the optimum found. In the presence of constraints, the optimality conditions are the Karush–Kuhn–Tucker first- and second-order conditions [62,63]. Global deterministic algorithms have some disadvantages that restrict their scope or hinder application in practice. Thus, they usually require fulfilment of some conditions that cannot be met or checked (*e.g.*, that the objective function and constraints be continuous and differentiable). Also, virtually no existing method affords detection of the global optimum for a problem within a finite length of time [64].

On the other hand, stochastic methods use no systematic procedure to determine search directions; rather, they use probabilistic methodology with a substantial heuristic slant and rarely consider structural information about the problem concerned. Their random nature usually precludes convergence on the optimum —many methods, however, provide asymptotic evidence of convergence. Usually, the likelihood of the optimum being reached approaches unity as the number of algorithm iterations grows.

There are several excellent reviews of the different types of optimization problems addressed in process engineering and the methods typically used to solve them [65,66].

1.2.2. Deterministic optimization methods

The local —largely deterministic— methods for this purpose can be of the direct type, which only require calculating the objective function, or indirect type, which require

using both the gradient and Hessian of this. Worth special note among the direct methods are the Simplex [44], the Complex [67], and those of Hooke *et al.* [48]. On the other hand, the most popular methods of the indirect type are *quasi*-Newton methods (particularly BFGS [62]), the conjugate gradient method [48], the Levenberg–Marquardt algorithm [68,69], Sequential Quadratic Programming (SQP) methods [48,70–73] and Generalized Reduced Gradient (GRG) methods [74].

The deterministic global algorithms used in this context include enumerative, successive approximation and successive division methods. The most popular enumerative methods are extreme point ranking [75] and cutting plane methods [76,77]. Successive approximation methods can be of the outer approximation (OA) [78], inner approximation [79] or successive underestimation type [80], among others. Finally, successive division methods, which are also known as "branch and bound" methods, include interval methods [81–83] and, especially, the αBB algorithm [84–91], which has successfully solved various chemical engineering design and control problems [92–94].

1.2.3. Stochastic optimization methods

Stochastic global algorithms can be classified as adaptive stochastic methods [95,96], the best-known among which is that based on Controlled Random Search (CRS) [97,98]; clustering methods [99,100]; evolutionary computation methods (also known as "bioinspired" methods) [101]; Simulated Annealing (SA) methods; and heuristic methods (particularly those based on Tabu Search, TS, and Ant Colonies, ACO) [102-106].

Bioinspired methods have so far been the most widely used stochastic global algorithms on account of their high efficiency and ease of application. Bioinspired methods rely on genetic algorithms (GA) [107–109], evolutionary programming (EP) [110] or

evolutionary strategies (ES) [111–114] depending on the particular type of variable (binary or real) used to represent individuals in implementing cross-over and mutation operators, and on the abstraction level used (genes with GA, individuals with ES and species with EP). As a rule, evolutionary computation methods are highly efficient and robust for solving a wide range of optimization problems (*e.g.*, estimating the parameters of a dynamic model); also, they require imposing virtually no constraints on the objective function or additional restrictions and are very easy to implement. In addition, they allow available knowledge about the problem at hand to be easily incorporated and hyphenated techniques to be used in order to overcome some shortcoming of purely evolutionary techniques such as slow convergence in the vicinity of the global optimum [60].

In summary, estimating the parameters of a model is rather a complex problem depending on its particular structure, the structural identifiability [115], the quality of available experimental data and potential correlation between parameters, among other factors. As stated above, stochastic global methods in general, and those based on an evolutionary approach in particular, are seemingly the best suited to the problem addressed in this work. In any case, this assumption is justified in greater detail later on.

2. Experimental section

Although the materials and methods used are described in part I, a brief summary of the operating conditions employed in all tests is provided here for better understanding of the subsequent discussion. Such conditions were as follows:

(a) Semi-continuous operation.

(b) Wine containing 93 g ethanol·L^{-1} as raw material.

(c) A constant temperature of 31 ºC.

(d) An air flow-rate of 7.5 L air·L^{-1} medium·h^{-1} with the fermenter loaded to the full working volume (8 L).

(e) A feed rate of 0.035 L·min^{-1}.

These conditions were used in two series of experiments, namely:

(a) A1, A2 and A3, which involved unloading the fermenter to a variable extent (75 %, 50 % and 25 %, respectively, of the total working volume) between cycles. The ethanol concentration at unload, however, was identical [15.5 g·L^{-1}] in all cases.

(b) B1, B2 and B3, which involved variable concentrations of ethanol at unload [27.1, 15.5 and 3.9 g·L^{-1}, respectively]. The unload volume was identical (50 %) in all cases.

The most salient results of these tests, and the average acetification rate obtained in each [116], are described in detail in part I.

In addition, the proposed model was validated in four tests under conditions other than those used for parameter estimation, namely:

(a) In test C1, 75 % of the fermenter volume was unloaded [to an ethanol concentration of 3.9 g·L^{-1}] and then continuously fed with 93 g ethanol·L^{-1} wine at a flow-rate of 0.01 L·min^{-1}.

(b) Test C2 the fermenter was unloaded by 25 % [to an ethanol concentration of 27.1 g·L^{-1}] and then continuously fed with 93 g ethanol·L^{-1} wine at a flow-rate of 0.06 L·min^{-1}.

(c) In test C3, the fermenter was unloaded by 50 % [to an ethanol concentration of 11.6 g·L^{-1}] and fed with 93 g ethanol·L^{-1} wine at 0.02 L·min^{-1} while keeping the ethanol concentration constant at *ca.* 38.8 g·L^{-1}.

(d) Finally, in test C4, the fermenter was unloaded to 50 % [to an ethanol concentration of 3.9 $g \cdot L^{-1}$] and then fed with 93 g ethanol$\cdot L^{-1}$ wine at 0.02 $L \cdot min^{-1}$ at a constant ethanol concentration in the region of 38.8 $g \cdot L^{-1}$.

3. Results and discussion

3.1. Ranges of variation of the model parameters

Before practical identifiability and parameter estimation was addressed, the potential ranges of variation of the model parameters were assesed. To this end, the performance of the different kinetic equations proposed in part I was examined under the following constraints:

(a) The parameters were only allowed to take positive values.

(b) Those parameter values leading to outputs beyond the lower or upper bound for the respective kinetic functions were rejected.

(c) Wherever possible, those parameter values lacking physical meaning as per the experimental concentration ranges spanned by the substrates and products were also be rejected.

In the proposed model, the specific growth rate, μ_c, depends on three factors (f_e, f_a and f_o) ranging from 0 to 1, and on its maximum possible value (μ_{max}). The latter has a zero lower bound but, initially, lacks an upper bound. Therefore, μ_{max} can in theory span the mathematical range $\mu_{max} \in]0, \infty[$. However, the upper bound can be reasonably set at 2 h^{-1}, which is the maximum typical value for a number of bacteria in the absence of growth limitation and inhibition. The expression for f_e depends on the ethanol concentration as well as on K_{SE} and K_{IE}. By analogy with the well-known Monod equation, parameter K_{SE} is a measure of growth limitation caused by an ethanol

deficiency. A low K_{SE} value suggests that the microbes can continue to grow at their maximal rate even in the presence of a low substrate concentration in the medium. Based on the ethanol uptake rate during the production stage in each cycle, microbial activity remains unaffected unless the ethanol concentration falls to levels below about 7.8 g·L^{-1}. This suggests that the upper bound for K_{SE} is about 10 g ethanol·L^{-1}. On the other hand, K_{IE} is a measure of bacterial sensitivity to the inhibitory effect of ethanol in the medium. Thus, a low value of K_{IE} must reflect strong inhibition by the substrate and a high value the opposite effect. While the lower bound for K_{IE} can easily be near-zero, there is no unambiguous indication as to what its upper bound may be. In fact, the careful analysis of the f_e function and inspection of the simulation at a selected K_{SE} value made by way of example in Figure 1 clearly reveal that the inhibitory effect of the substrate decreases with increase in K_{IE}. Therefore, the convenience of using as clearly bound ranges as possible for each parameter in its estimation led us to choose a value coinciding with the highest concentration potentially obtained in the fermentation cycles (*ca.* 90 g ethanol·L^{-1}).

< Figure 1 >

The proposed expression for f_a depends on the acetic acid concentration and also on an inhibition constant (K_{IA}). This parameter can be assumed to represent the sensitivity of the bacterial population to the acetic acid concentration in the medium. Since the dimensions of K_{IA} coincide with those of the acetic acid concentration, its variation range can reasonably be identified with that of acid concentrations potentially found in the medium. Figure 2 shows the variation of f_a with the acetic acid concentration at different K_{IA} values. As with f_e, no unambiguous information exists to set an upper

bound for f_a. We thus chose to identify it with the highest acetic acid concentration found in the experimental tests (*ca.* 120 g·L^{-1}). As can be seen from Figure 2, relatively low values of K_{IA} result in excessively strong inhibition —even at acetic acid concentrations known to cause no such effect—; therefore, the potential range of variation for this parameter should exclude such low K_{IA} values. In summary, based on the experimental results, the lower bound for K_{IA} could be in the region of 60 g acetic acid·L^{-1}.

< Figure 2 >

The proposed expression for f_o has the typical structure of a Monod equation. Therefore, K_{so} represents the dissolved oxygen concentration at which the function has one-half of its maximum possible value. Nieto [117] examined the sensitivity of bacterial growth to oxygen availability in the medium and found cell growth to drop at a dissolved oxygen concentration that was dependent on the acidity of the medium. Thus, dissolved oxygen levels in the range 0.5–1.5 mg·L^{-1} reduced the bacterial growth rate to roughly one-half the maximum possible levels in the presence of acid concentrations from 60 to 100 g·L^{-1}. Based on these results, K_{SO} may adopt values within the previous oxygen concentration range. However, we chose to use 0 and 1.5 mg oxygen·L^{-1} as the lower and upper bound, respectively, and hence a broader range in order to increase freedom in the estimation algorithm to be subsequently applied in the determination of the optimum parameter value while checking that the fitting provided values no just at the range limits.

The kinetic expressions for cell death include three parameters, namely: μ_d^0, K_{mA} and K_{mE}. Functions f_{dE} and f_{dA}, which contain parameters K_{mE} and K_{mA}, were not limited to a unity value —in fact, they should always exceed 1 by virtue of their mathematical

structure— since some culture conditions can lead to additional cell death and to the cell death rate, μ_d^0, being exceeded. Therefore, no such constraint was imposed on the functions in determining the practical bounds for the corresponding parameters.

As will cell growth, only the lower bound (zero) was known for μ_d^0 as it had no upper bound in theory. As with μ_{max}, however, there are some practical limits for the specific cell death rate which, in the absence of additional information, can be identified with those for μ_{max}, namely: 0 and 1.5–2 h^{-1}.

As far as K_{mE} is concerned, f_{dE} changes monotonically with the ethanol concentration, the variation profile depending on this parameter. Figure 3 illustrates the effect of various K_{mE} values on f_{dE}. Similarly as before, no conclusive criterion for setting the upper bound for this parameter exists, which led us to initially identify it with the highest ethanol concentration obtained in the fermentation cycles (90 g·L^{-1}). Likewise, the figure suggests a vast effect of too low a K_{mE} value on cell death, one that is hardly realistic as can be easily checked through testing. In any case, we chose to use a lower bound of 10 g ethanol·L^{-1} in order to avoid excessively restricting the variation range for this parameter.

< Figure 3 >

The reasoning for parameter K_{mA} is similar to that made for K_{mE}. Its lower and upper bound were chosen to be 10 and 120 g acetic acid·L^{-1}, respectively. Figure 4 shows a simulation of the f_{dA} function at different K_{mA} values.

< Figure 4 >

Finally, the proposed expression for the lysis kinetics contains a single parameter, μ_{lysis}, the lower and upper bound for which can be identified with those for μ_{max} and μ_d^0 (*viz.*, 0 and 2 h^{-1}, respectively).

By way of summary, Table 1 shows the model parameters and their respective lower and upper bounds.

Parameter	Bounds
μ_{max}	[0, 2] h^{-1}
K_{SE}	[0, 10] g ethanol·L^{-1}
K_{IE}	[0.25, 90] g ethanol·L^{-1}
K_{IA}	[20, 120] g acetic acid·L^{-1}
K_{SO}	[0, 1.5]·10^{-3} g oxygen·L^{-1}
μ_d^0	[0, 2] h^{-1}
K_{mE}	[10, 90] g ethanol·L^{-1}
K_{mA}	[10, 120] g acetic acid·L^{-1}
μ_{lysis}	[0, 2] h^{-1}

Table 1: Lower and upper bounds of the variation ranges for the model parameters

3.2. Practical identifiability analysis and parameter estimation

The practical identifiability of the model was assessed and its parameters estimated from the results of tests A1–A3 and B1–B3. The analysis was performed separately for each test and the results compared at a later stage in order to establish a unique parameter set. Then, the model was validated with the ensuing parameters, using the data from tests C1–C4. Validation involved comparing the simulated outputs of the model with such data and analysing the residuals.

The former analysis was done by using an improved iterative procedure for selecting identifiable parameters based on FIM characteristics [22]. This procedure uses a starting value for each parameter that can be obtained from the literature or from past experience. In this work, we used a sub-optimal value estimated with a stochastic global algorithm (specifically, an evolutionary strategy, ES). Such an algorithm has been used for the following reasons:

(a) No starting values for the parameters were available. In fact, the sole information on them was their approximate range of variation.

(b) The algorithm allowed a point near the potential optimum in the parameter space to be located, thereby facilitating convergence and reducing the number of iterations needed as a result.

(c) The multi-modal, non-convex nature of the problem required using a global optimization method.

(d) The chosen algorithm was subject to no special constraint as regards the objective function and restrictions, and allowed the problem to be addressed as a black-box one.

(e) The algorithm provided a robust method featuring computation times usually much shorter than those of alternative procedures.

The specific procedure used was an evolutionary strategy known as the "Augmented Lagrangian Genetic Algorithm" (ALGA) [118,119], which affords solving NLP problems with equality and inequality constraints, and subject to upper and lower bounds for the decision variables. Once a sub-optimum was found, a local deterministic optimization algorithm with constraints was applied to the parameters exhibiting the highest practical identifiability in each case as decision variables in order to improve the solution. The specific procedure used for this purpose was an SQP algorithm.

The numerical integration of the model was done with the DASSL algorithm [36], using the EcosimPro modelling and simulation environment [120].

3.2.1. Detailed analysis for experiment A1

A comprehensive description of the analysis for test A1 follows. The procedure used with the other estimation tests (A2, A3 and B1–B3) was identical, but only their final outputs are shown here for brevity.

The experimental data were obtained in 8 fermentation cycles. The data include the concentrations of viable cells, total cells, ethanol and acetic acid. Cell concentrations were determined as described elsewhere [121].

Based on the following arguments, the experimental data were assumed to be roughly normally distributed:

(a) Means and medians were virtually identical at any point in time. Also, the symmetry or bias coefficient [122] tended to zero; therefore, the sample distribution was roughly symmetric.

(b) As shown by the Kolmogorov–Smirnoff test at the 95 % confidence level, the sample was normally distributed.

In addition, the measurement sequence was checked to be homoscedastic, *i.e.*, the probability distribution of all measurements was subject to approximately the same standard deviation (about 0.8 $g \cdot L^{-1}$ for the ethanol concentration and *ca.* 0.02 $g \cdot L^{-1}$ for both the total and viable cell concentrations). All these findings were also applied to measurement errors, which were also assumed to be normally distributed —with a zero mean, however— and possess identical standard deviations. Also, we assumed output measurements to be independent from one another as their data collection fulfilled the sufficient condition of physical independence.

Based on the foregoing, we obtained the following measurement error covariance matrix:

$$Q = \begin{bmatrix} 4.1311 \cdot 10^{-4} & 0 & 0 \\ 0 & 4.1311 \cdot 10^{-4} & 0 \\ 0 & 0 & 0.6 \end{bmatrix} \quad (1)$$

which was used as a weight for the weighted least-squares function in addition to another weight intended to offset differences in order of magnitude between measurements. Such a weight was 10^3 and applied to cell concentrations only.

The next step was to estimate the parameter models, focusing on minimizing this objective function, and including the model equations and the previously established lower and upper bounds for the parameter values (Table 1) as constraints for the problem. Optimization was done with the above-described ALGA method, which was set to operate as follows:

(a) The population used in each generation consisted of 20 individuals.

(b) The parent individuals for the next generation were selected by using a uniform stochastic mechanism.

(c) Two elite individuals —the best parents— in each generation were directly transferred to the next.

(d) Each generation was obtained by cross-over (80%) and mutation (20%) from the previous one.

(e) The recombination mechanism started from a random binary vector of identical length as the genetic code of each individual. Then, the algorithm parsed the vector: when it met a 1 bit, it adopted the gene (*viz.*, the value of the decision variable) from the first parent in that position; otherwise (*i.e.*, if it met a 0 bit), then it adopted the gene from the second parent. This allowed the genetic code of each child to be assembled.

(f) Mutation was done by using an appropriate algorithm to randomly generate mutation directions the step length of which was chosen in such a way as to ensure fulfilment of the previously established constraints.

(g) The initial value of the quadratic penalty function was 10 and the penalty factor 100. The latter increased the parameter value when the problem was inadequately precisely solved as regards tolerance of the objective function and the constraints.

The stop criteria used with the evolutionary strategy included the following:

(a) Tolerance of the function: the algorithm stopped when the ratio of the weighted mean change in the objective function to the maximum number of stall generations (*viz.*, those resulting in no progress of the objective function) fell below 10^{-15}.

(b) Maximum number of generations: the algorithm stopped when the number of generations exceeded 5000.

(c) Maximum stall time: the algorithm stopped if successive generations produced over a period of 300 s resulted in no progress of the objective function.

Figure 5 provides a conceptual scheme for the overall parameter estimation strategy.

< Figure 5 >

The stochastic nature of the strategy led to perform a total of 100 estimations and choose the best output in terms of the objective function. The parameter values thus obtained are listed in Table 2.

Parameter	Value
μ_{max}	0.62 h^{-1}
K_{SE}	3.8 g ethanolL^{-1}
K_{IE}	10.63 g ethanol·L^{-1}
K_{IA}	98.6 g acetic acid·L^{-1}
K_{SO}	$3.33 \cdot 10^{-4}$ g oxygen·L^{-1}
μ_d^0	$2.94 \cdot 10^{-5}$ h^{-1}
K_{mE}	36.81 g ethanol·L^{-1}
K_{mA}	12.51 g acetic acid·L^{-1}
μ_{lysis}	0.52 h^{-1}

Table 2: Parameter values obtained by applying ALGA to the results of test A1

A value of 1893.2 was thus obtained for the objective function. Figure 6 compares the experimental data (circle marker) with the outputs provided by the parameter set of Table 2 (dashed line).

< Figure 6 >

As can be seen, except for the oxygen, the fit was quite good the result must be very close to the actual optimum.

The observed fitting for solved oxygen concentration might be explained taking into account that, in the used bioreactor the gas phase undergoes no thorough mixing, so nearby the input for air a higher gas volume fraction than in other parts can be found (the oxygen probe is placed in this zone); on the other hand, the low surface tension in the culture medium leads to complex interfacial phenomena such as (for instant) a decrease in coalescence of the bubbles formed in the device used to disrupt the incoming air stream affecting the interfacial area [123]. So, in our opinion, both facts affect the oxygen probe readings showing values higher than those existing in the liquid phase.

Therefore, values for the parameter set constituted an effective starting point for a practical identifiability analysis. The core of such an analysis was calculating the sensitivity functions for the cell and ethanol concentrations by using the previously determined parameter values. In figures 7-9 the instantaneous percentages of variation of such functions are plotted. One immediate inference from the three is that parameters K_{SE} and K_{IA} had virtually no influence on any output (see scales on those figures), but especially on cell concentrations; also, μ_{lysis} had no effect on the variation of the concentrations of viable cells or ethanol, and only a minimal effect on the total cell concentration. On the other hand, K_{SO} and μ_d^0 exhibited a strong influence on all outputs (particularly μ_d^0).

< Figure 7 >

< Figure 8 >

< Figure 9 >

The mere visual inspection of these figures confirms some of our previous conclusions. Thus, all outputs were virtually insensitive to K_{SE} and K_{IA}. Also, μ_{lysis} had no effect on X_v or E, and only a slight influence on X —the corresponding sensitivity functions amounting to *ca.* 20 % of the concentration at some points in time. Therefore, the total cell concentration can be informative enough to estimate this parameter. As can also be seen from the figures, K_{mE} had little influence on any output —about 5 % at most on X_v and X, and approximately 2 % at most on E—; therefore, the model is scarcely sensitive to this parameter —albeit slightly more so than to the others.

In addition, the variation of the sensitivity functions for X_v and X was similar for all parameters except μ_{lysis}. This was a result of X_v being roughly a fraction of the total cell concentration, X, virtually throughout the cycle, and the two outputs being somewhat proportional as a result. However, cell lysis only influenced the latter concentration as it affected the concentration of non-viable cells, but not that of viable cells. In summary, both concentrations are needed to estimate the whole parameter set.

As can be seen from Figures 7–9, the sensitivity functions for some parameter couples exhibited a roughly identical profile for all outputs, which suggests the presence of substantial correlation between parameters. Should this finding be confirmed, different combinations of parameter values might lead to virtually identical experimental results.

The FIM rank was calculated to be 9; therefore, the model parameters were not completely unidentifiable. Based on some previous comments, however, the model was poorly identifiable around the point in the parameter space determined under the

experimental conditions used owing to the virtually non-existent influence of some parameters and the apparent correlations between others.

In order to confirm this assumption, we applied the selection procedure to a set comprising the most practically identifiable parameters [22], using 0.5 as upper bound for the absolute correlation value for each parameter combination. However, the procedure was slightly modified by excluding the exceedingly uninfluential parameters detected through inspection of the sensitivity functions from the studied combinations. This modification was imposed by the fact that the D-optimal criterion used to identify parameter combinations meeting the maximum correlation criterion (*viz.*, the product of the eigenvalues of the Fisher Information Matrix) had the disadvantage that multiplying very low values for poorly influential parameters and very high values ones for strongly influential ones yielded too high index values in some cases. This in turn might lead to deeming identifiable combinations including some uninfluential parameter by effect of the algorithm output being a combination containing one or more practically unidentifiable parameters. The modification used efficiently circumvented this shortcoming.

In the first iteration, the algorithm constructed every possible combination containing between two parameters and their total number — K_{SE} and K_{IA} excluded on the grounds of their above-mentioned scant influence on the model outputs. This provided a range of combinations including 2–7 parameters. Table 3 shows the most identifiable among them at a preset maximum correlation level (first column) and the actual maximum correlations (fourth column).

Correlation limit	**Parameter combination**	**D-optimal criterion**	**Maximum correlation for the combination**

0.5	K_{SO}, μ_{lysis}	$3.0212 \cdot 10^{13}$	–0.171
0.6	μ_d^0, μ_{lysis}	$1.3087 \cdot 10^{16}$	–0.5073
0.65	Same result as for the correlation limit: 0.6		
0.7	Same result as for the correlation limit: 0.6		
0.75	Same result as for the correlation limit: 0.6		
0.8	μ_{max}, μ_d^0	$1.8269 \cdot 10^{19}$	0.7836
0.85	K_{SO}, μ_d^0	$6.2301 \cdot 10^{23}$	–0.8129
0.9	K_{SO}, μ_d^0, μ_{lysis}	$1.9432 \cdot 10^{26}$	–0.8552

Table 3: Combinations of the most identifiable parameters in the first iteration for test A1

As can be seen from the table, only two binary parameter combinations (viz., $K_{SO} - \mu_{lysis}$ and $\mu_d^0 - \mu_{lysis}$, with a maximum correlation of –0.171 and –0.5073) were practically identifiable at a maximum correlation limit of 0.5. Therefore, the model, as formulated, not only contains rather uninfluential parameters (K_{SE} and K_{IA}), but also, as previously inferred from the sensitivity functions, exhibits strong correlation between others. We chose the latter combination ($\mu_d^0 - \mu_{lysis}$) as the more identifiable as it exhibited an absolute correlation very close to 0.5 and a D-optimal criterion 1000 times greater than the former —this should result in more precise parameter estimation or, in other words, in more accurate determination of the biased optimum of the objective function.

The next step involved improving the solution by estimating the previously selected most identifiable parameters. The solution in question would be biased by the other parameters, which were kept constant at the values determined with the evolutionary strategy. The estimation procedure used was a local deterministic optimization algorithm affording management of constraints. Therefore, the overall strategy was of the hybrid type (first global and then local). Its use provided the next results: $\mu_d^0 = 2.6 \cdot 10^{-5}\ \mathrm{h}^{-1}$ and $\mu_{lysis} = 0.49\ \mathrm{h}^{-1}$.

The value of the objective function thus obtained was 1229.6, which is smaller than the earlier calculation. Obviously, the estimations were biased by the effect of excluded parameters.

Repeating the whole process with the new parameter set led to the same results, *i.e.*, the ensuing sensitivity functions were very similar to those of Figures 7–9 and the most identifiable parameters were again μ_d^0 and μ_{lysis}. Therefore, no further iteration was required and the process was finished by adopting the parameter values shown in column A1 of Table 4 as optimal for this experiment. Practical identifiability, however, is rather difficult to estimate from available data obtained under these experimental conditions.

Figure 6 also shows the model outputs obtained with the optimal parameter values (solid line) together with those provided by the initial values (dashed line) and the experimental data used (circle marker). As can be seen from the figure, these parameter values allowed the model to reproduce the experimental results quite closely.

Figure 10 shows the residuals (*viz.*, the differences between model outputs and experimental data) obtained with the optimal parameter vector; as can be seen, they were randomly distributed around zero (*i.e.*, they had a zero mean). On the other hand, their standard deviations are very similar to the corresponding measurement errors (0.02 $g \cdot L^{-1}$ in cell concentrations and 0.78 $g \cdot L^{-1}$ in the ethanol concentration). Consequently, the model can be assumed to provide accurate predictions, and the fitting to be roughly optimal, under these experimental conditions. However, the parameter values afford no reliable conclusion as regards physical meaning since the model provides a biased solution.

< Figure 10 >

3.2.2. Analysis for experiments A2, A3, B1 and B3

As with A1, application of the same procedure to the results of tests A2, A3 and B1–B3 afforded no complete practical identifiability. The optimal parameter sets thus obtained are shown in Table 4. As in the case of the experiment A1, the experimental data were optimally fitted in all tests.

In order to obtain a unique value for each parameter, these data were used to determine average parameter values which provide a parameter set shown in last column of Table 4. Obviously, these mean parameter values resulted in highly accurate reproduction of all experimental results.

	A1	A2	A3	B1	B3	**Mean**
μ_{max} (h^{-1})	0.62	0.61	0.61	0.62	0.61	0.61
K_{SE} (g ethanol·L^{-1})	3.8	3.64	3.55	3.59	4.06	3.73
K_{IE} (g ethanol·L^{-1})	10.63	10.82	11.16	9.92	11.97	10.9
K_{IA} (g acetic acid·L^{-1})	98.6	97.66	103.29	97.23	103.93	100.14
K_{SO} (g oxygen·L^{-1})	$3.33\cdot10^{-4}$	$3.18\cdot10^{-4}$	$3.31\cdot10^{-4}$	$3.2\cdot10^{-4}$	$3.39\cdot10^{-4}$	$3.28\cdot10^{-4}$
μ_d^0 (h^{-1})	$2.6\cdot10^{-5}$	$2.53\cdot10^{-5}$	$2.55\cdot10^{-5}$	$2.08\cdot10^{-5}$	$3.04\cdot10^{-5}$	$2.56\cdot10^{-5}$
K_{mE} (g ethanol·L^{-1})	36.81	38.01	37.54	38.26	37.53	37.63
K_{mA} (g acetic acid·L^{-1})	12.51	12.13	13.02	12.98	12.81	12.69
μ_{lysis} (h^{-1})	0.49	0.46	0.48	0.48	0.49	0.48

Table 4: Optimum parameter values obtained in different tests

3.3. Model validation

The last step in the process involved validating the model by using experimental results obtained under conditions other than those employed in its construction (*viz.*, tests C1–

C4). Figures 11–14 compare the resulting simulated outputs in graphical form. Based on them, the proposed model is valid within the operational range established from the experimental tests conducted here. Therefore, it may be of use in other types of studies involving the use of models for predictive purposes.

< Figure 11 >

< Figure 12 >

< Figure 13 >

< Figure 14 >

4. Conclusions

In part II of this series we simultaneously addressed the practical identifiability and estimation of the parameters of the model for acetic acid fermentation proposed in part I. This type of study, though it should always be done, is unusual in Biochemical Engineering studies despite its high usefulness for accurate process modelling.

The most salient conclusion of our analysis is that none of the tests conducted afforded a practical identifiability analysis allowing the model parameters to be accurately obtained with any particular estimation algorithm. Thus, process outputs were poorly sensitive to some parameters (for instance, K_{SE} and K_{IA} have a influence lesser than 0.7 %) and strong correlations were detected between others (for instance, K_{SO}, μ_d^0 and μ_{lysis}, see table 3). Therefore, although the simulations reproduced the results of all tests —validation experiments included—, the outcome does not allow one to attach physical meaning to the parameters. In fact, the strong influence of the quality of the experimental data used on the outcome of the parameter identifiability analysis entails carefully designing the experimental testing for optimal results.

The practical identifiability analysis was approached with a strategy of local type based on inspection of the sensitivity functions and an iterative procedure which afforded pin-pointing of the most identifiable parameters around a given point in the parameter space by determining the parameter estimation correlation matrix with exclusion of those parameters scarcely influencing the outputs. The local nature of this approach entailed estimating the model parameters; therefore, the point around which the analysis was conducted in each iteration was a sub-optimum provided by an optimization algorithm (an evolutionary strategy known as ALGA). This facilitated convergence in selecting the most identifiable parameters (those combinations with a correlation lower than 0.5) and simultaneously improving the solution. If one or more parameters are inadequately identifiable —as some in the studied model indeed were—, then the solution will be biased by effect of the parameters retaining fixed nominal values.

Parameters were estimated by using a hybrid approach combining a stochastic global optimization algorithm (*viz.*, an evolutionary strategy) and a deterministic local algorithm (SQP). This choice was dictated by the low convergence rate of the former near the optimum, which was no hindrance with the latter. Therefore, the evolutionary strategy was used to determine the starting point for the parameter space to be used in the practical identifiability analysis, and the local method to gradually approach the potential global optimum. The evolutionary strategy proved quite an effective choice in this context; thus:

(a) it required no constraint to be imposed on the objective function or restrictions; and

(b) the computation time needed to obtain the objective function was reasonably short —it never exceeded 20–25 minutes on a standard PC. Despite their stochastic nature, evolutionary strategies and related

algorithms are much more expeditious than alternative procedures in practice.

So, the estimated parameter values were: μ_{max}=0.61 h^{-1}, K_{SE}=3.73 g ethanol·L^{-1}, K_{IE}=10.9 g ethanol·L^{-1}, K_{IA}=100.14 g acetic acid·L^{-1}, K_{SO}=3.28·10^{-4} g oxygen·L^{-1}, μ_d^0=2.56·10^{-5} h^{-1}, K_{mE}=37.63 g ethanol·L^{-1}, K_{mA}=12.69 g acetic acid·L^{-1} and μ_{lysis}=0.48 h^{-1}.

Finally, the model provides quite an accurate reproduction not only of the experimental results used to estimate its parameters, but also of a series of validation tests performed under alternative conditions. Therefore, the proposed model can also be useful for other problems falling within the scope of the body of tests used (e.g., dynamic optimization of the process).

5. References

[1] D.R. Nielsen, A.J. Daugulis, P.J. McLellan, Dynamic simulation of benzene vapour treatment by a two-phase partitioning bioscrubber. Part 1: Model development, parameter estimation and parametric sensitivity, Biochem. Eng. J. 36 (2007) 239–249.

[2] N. Noykova, Modelling and identification of microbial population dynamics in wastewater treatment, PhD Thesis (2002), University of Turku, Finland.

[3] P. Kesavan, V.J. Law, Practical identifiability of parameters in Monod kinetics and statistical analysis of residuals, Biochem. Eng. J. 24 (2005) 95–104.

[4] R.A. Fisher, On an absolute criterion for fitting frequency curves, Mess. Math. 41 (1912) 155–160.

[5] A. Munack, Optimal feeding strategy for identification of Monod-type models by fed-batch experiments. In N.M. Fish, R.I. Fox, N.F. Thornhill (Ed.), Computer

Applications in Fermentation Technology Modelling and Control of Biotechnological Processes, Elsevier (1989) 195–204.

[6] E. Walter, L. Pronzato, Qualitative and quantitative experiment design for phenomenological models –a survey, Automatica 26 (1990) 195–213.

[7] A. Munack, Optimization of sampling. In K. Schügerl (Ed.), Biotechnology, a multi-volume comprehensive treatise. Vol. 4: Measuring, modelling and control, VCH (1991) 252–264.

[8] P.A. Vanrolleghem, D. Dochain, Bioprocess model identification. In J.F.M. Van Impe, P.A. Vanrolleghem, D. Iserentant, (Eds.), Advanced instrumentation, data interpretation and control of biotechnological processes, Kluwer Academic Publishers (1998) 251–318.

[9] L. Ljung, System identification. Theory for the user, Prentice–Hall (1999).

[10] D. Dochain, P.A. Vanrolleghem, Dynamical modelling and estimation in wastewater treatment processes, IWA Publishing (2001).

[11] A. Holmberg, On the practical identifiability of microbial growth models incorporating Michaelis–Menten type nonlinearities, Math. Biosci. 62 (1982) 23–43.

[12] K.J. Versyck, J.E. Claes, J.F. Van Impe, Practical identification of unstructured growth kinetics by application of optimal experimental design, Biotechnol. Prog. 13 (1997) 524–531.

[13] K.J. Keesman, H. Spanjers, G. van Straten, Analysis of endogenous process behaviour in activated sludge, Biotech. Bioeng. 57 (1998) 155–163.

[14] M.E. Hidalgo, E. Ayesa, Numerical and graphical description of the information matrix in calibration experiments for state–space models, Wat. Res. 35 (2001) 3206–3214.

[15] B. Petersen, K. Gernaey, P.A. Vanrolleghem, Practical identifiability of model parameters by combined respirometric–titrimetric measurements, Wat. Sci. Technol. 43 (2001) 347–355.

[16] P. Reichert, P.A. Vanrolleghem, Identifiability and uncertainty analysis of the river quality model No.1 (RWQM1), Wat. Sci. Technol. 43 (2001) 329–338.

[17] T.G. Müller, N. Noykova, M. Gyllemberg, J. Timmer, Parameter identification in microbial population dynamics models of anaerobic waste water treatment processes with substrate inhibition, Biopr. Eng. 23 (2002) 343–349.

[18] N. Noykova, T. Müller, M. Gyllenberg, J. Timmer, Quantitative analysis of anaerobic wastewater treatment processes: identifiability and parameter estimation, Biotech. Bioeng. 78 (2002) 89–103.

[19] S.T. Yordanova, N. Noykova, Influence of perturbations on the wastewater treatment process, Chem. Biochem. Eng. Q. 10 (1996) 9–14.

[20] N. Noykova, M. Gyllemberg, Sensitivity analysis and parameter estimation in a model of anaerobic waste water treatment processes with substrate inhibition, Biopr. Eng. 23 (2000) 343–349.

[21] S.R. Weijers, J.J. Kok, H.A. Preisig, A. Buunen, T.W.M. Wouda, Parameter identifiability of IAWQ model no. 1 for modelling activated sludge plants for enhanced nitrogen removal, Comput. Chem. Eng. 20 (1996) S1455–1460.

[22] D. De Paw, Optimal experimental design for calibration of bioprocess models: a validated software toolbox, PhD Thesis (2005). University of Ghent, The Netherlands.

[23] R. Brun, P. Reichert, H.R. Kunsch, Practical identifiability analysis of large environmental simulation models, Water Resour. Res. 37 (2001) 1015–1030.

[24] K.J. Versyck, J.E. Claes, J. Van Impe, Optimal experimental design for practical identification of unstructured growth models, Math. Comput. Simul. 46 (1998) 623–631.

[25] K.J. Versyck, K. Bernaerts, A.H. Geeraerd, J. Van Impe, Introducing optimal experimental design in predictive modelling: a motivating example, Int. J. Food Microbiol. 51 (1999) 39–51.

[26] J.R. Banga, K.J. Versyck, J.F. Van Impe, Computation of optimal identification experiments for nonlinear dynamic process models: a stochastic global optimization approach, Ind. Eng. Chem. Res. 41 (2002) 2425–2430.

[27] K. Bernaerts, R.D. Servaes, S. Kooyman, K.J. Versyck, J.F. Van Impe, Optimal temperature input design for estimation of the Square Root model parameters: parameter accuracy and model validity restrictions, Int. J. Food Microbiol. 73 (2002) 145–157.

[28] R.W. Atherton, R.B. Schainker, E.R. Ducot, Statistical sensitivity analysis of models for chemical-kinetics, AIChE Journal 21 (1975) 441–448.

[29] J.T. Hwang, E.P. Dougherty, S. Rabitz, H. Rabitz, The Green's function method of sensitivity analysis in chemical kinetics, J. Chem. Phys. 69 (1978) 5180–5191.

[30] J.T. Hwang, Sensitivity analysis in chemical kinetics by the method of polynomial approximations, Int. J. Chem. Kinet. 15 (1983) 959–987.

[31] J.T. Hwang, A computational algorithm for the polynomial approximation method of sensitivity analysis in chemical kinetics, J. Chin. Chem. Soc-Taip 32 (1985) 253–261.

[32] D. Hwang, D.W. Brun, M.T. Odman, An automatic differentiation technique for sensitivity analysis of numerical advection schemes in air quality models, Atmos. Environ. 31 (1997) 879–888.

[33] J.R.R.A. Martins, P. Sturdza, J.J. Alonso, The complex-step derivative approximation, ACM T. Math. Software 29 (2003) 245–262.

[34] W. Squire, G. Trapp, Using complex variables to estimate derivatives of real functions, SIAM Rev. 40 (1998) 110–112.

[35] A. Hindmarsh, ODEPACK, a systematized collection of ODE solvers. In R. Stepleman, (Ed.), Scientific Computing, North Holland (1983) 55–64.

[36] K.E. Brenan, S.L. Campbell, L.R. Petzold, Numerical solution of initial-value problems in differential-algebraic equations, Elsevier Science Publishers (1989).

[37] J.V. Beck, K.J. Arnold, Parameter estimation in engineering and science, John Wiley & Sons (1997).

[38] W. Spendley, G.R. Hext, F.R. Himsworth, Sequential applications of simplex designs in optimisation and evolutionary operation, Technometrics 4 (1962) 441–461.

[39] J.A. Nelder, R. Mead, A simplex method for function minimization, Comput. J. 7 (1965) 308–313.

[40] W.H. Press, S.A. Teukolsky, W.T. Vetterling, B.P. Flannery, Numerical recipes in C, Cambridge University Press (1992).

[41] J.N. Lyness, C.B. Moler, Numerical differentiation of analytic functions. SIAM J. Num. Anal. 4 (1967) 202–210.

[42] S. Marsili-Libelli, S. Guerrizio, N. Checchi, Confidence regions of estimated parameters for ecological systems, Ecol. Model. 165 (2002) 127–146.

[43] R. Fletcher, Practical methods of optimization, John Wiley & Sons (1987).

[44] G.A.F. Seber, C.J. Wild, Nonlinear regression, Wiley (1989).

[45] W. Horbelt, J. Timmer, W. Melzer, Estimating parameters in nonlinear differential equations with application to physiological data. In G. Osipenko (Ed.), Differential equations and applications (1998) 23–33.

[46] C.D. Knightes, C.A. Peters, Statistical analysis of nonlinear parameter estimation for Monod biodegradation kinetics using bivariate data, Biotech. Bioeng. 69 (2000) 161–170.

[47] H. Spanjers, G. Patry, K. Keesman, Respirometry-based on-line model parameter estimation at a full-scale WWTP, Wat. Sci. Technol. 45 (2002) 335–343.

[48] K.G. Gadkar, R. Gunawan, F.J. Doyle, Iterative approach to model identification of biological networks, BMC Bioinformatics 6 (2005) 155–175.

[49] R.C. Spear, G.M. Hornberger, Eutrophication in peel inlet. II. Identification of critical uncertainties via generalized sensitivity analysis, Water Res. 14 (1980) 43–49.

[50] K.J. Keesman, Membership-set estimation using random scanning and principal component analysis, Math. Comput. Simulat. 32 (1990) 535–543.

[51] K. Beven, A. Binley, The future of distributed models: model calibration and uncertainty prediction, Hydrol. Process. 6 (1992) 279–298.

[52] M. Omlin, P. Reichert, A comparison of techniques for the estimation of model prediction uncertainty, Ecol. Model. 115 (1999) 45–59.

[53] A. Abusam, K.J. Keesman, G. van Straten, H. Spanjers, K. Meinema, Parameter estimation procedure for complex nonlinear systems: calibration of ASM No. 1 for N-removal in a full-scale oxidation ditch, Water Sci. Technol. 43 (2001) 357–365.

[54] P. Reichert, R. von Schulthess, D. Wild, The use of aquasim for estimating parameters of activated sludge models, Water Sci. Technol. 31 (1995) 135–147.

[55] S.R. Weijers, P.A. Vanrolleghem, A procedure for selecting best identifiable parameters in calibrating activated sludge model No. 1 to full-scale plant data, Water Sci. Technol. 36 (1997) 69–79.

[56] S. Marsili-Libelli, P. Ratini, A. Spagni, G. Bortone, Implementation, study and calibration of a modified asm2d for the simulation of sbr processes, Water Sci. Technol. 43 (2001) 69–76.

[57] E.A. Seagren, H. Kim, B.F. Smets, Identifiability and retrievability of unique parameters describing intrinsic Andrews kinetics, Appl. Microbiol. Biot. 61 (2003) 314–322.

[58] K. Steppe, Diurnal dynamics of water flow through trees: design and validation of a mathematical flow and storage model, PhD Thesis (2004), University of Ghent, The Netherlands.

[59] R. Li, M.A. Henson, M.J. Kurtz, Selection of model parameters for off-line parameter estimation, IEEE Contr. Syst. Technol. 12 (2004) 402–412.

[60] C. Gutiérrez, Optimización global de procesos de la industria alimentaria y biotecnológica, PhD Thesis (2003), University of Vigo, Spain.

[61] E. Kostina, Robust parameter estimation in dynamic systems, Optim. Eng. 5 (2004) 461–484.

[62] M.S. Bazaraa, H.D. Sherali, C.M. Shetty, Nonlinear programming: theory and applications, John Wiley & Sons (1993).

[63] T.F. Edgar, D.M. Himmelblau, L. Lasdon, Optimization of chemical processes, McGraw–Hill (2001).

[64] C. Guus, E. Boender, H.E. Romeijn, Stochastic methods. In R. Horst, P.M. Pardalos, (Eds.), Handbook of global optimization, Kluwer Academic Publishers (1995).

[65] L.T. Biegler, I.E. Grossmann, Retrospective on optimization, Comput. Chem. Eng. 28 (2004) 1169–1192.

[66] I.E. Grossmann, L.T. Biegler, Part II. Future perspective on optimization, Comput. Chem. Eng. 28 (2004) 1193–1218.

[67] G.V. Reklaitis, A. Ravindran, K.M. Ragsdel, Engineering optimization: methods and applications, John Wiley & Sons (1983).

[68] K. Lebenberg, A method for the solution of certain non-linear problems in least-squares, Quart. Appl. Math. 2 (1944) 164–168.

[69] D.W. Marquardt, An algorithm for least-squares estimation of non-linear parameters, J. Soc. Ind. Appl. Math. 11 (1963) 431–441.

[70] K. Schittkowski, EASY-FIT: a software system for data fitting in dynamic systems, Struct. Multidiscip. O. 23 (2002) 153–169.

[71] M.J.D. Powell, Variable metric methods for constrained optimization, In A. Bachem, M. Grotschel, B. Korte, (Eds.), Mathematical programming: the state of the art, Springer–Verlag (1983), 288–311.

[72] P.T. Boggs, J.W. Tolle, Sequential quadratic programming, Acta Numer. (1995) 1–51.

[73] J. Nocedal, S. Wright, Numerical optimization, Springer (1999).

[74] E. Balsa, Algoritmos eficientes para la optimización dinámica de procesos distribuidos, PhD Thesis (2001), University of Vigo, Spain.

[75] K.G. Murty, Solving the fixed-charge problem by ranking the extreme points, Oper. Res. 16 (1968) 268–279.

[76] A.V. Cabot, Variations on a cutting plane method for solving concave minimization problems with linear constraints, Naval Res. Logist. Quart. 21 (1974) 265–274.

[77] R. Horst, H. Tuy, Global optimization: deterministic approaches, Springer–Verlag (1993).

[78] R. Horst, N.V. Thoai, Modification, implementation and comparison of three algorithms for globally solving linearly constrained concave minimization problems, Computing 42 (1989) 271–289.

[79] R. Horst, H. Tuy, Global optimization: deterministic approaches, Springer–Verlag (1990).

[80] J.E. Falk, K.L. Hoffman, A successive underestimating method for concave minimization problems, Math. Oper. Res. 1 (1976) 251–259.

[81] H. Ratschek, J. Rokne, Interval methods, In R. Horst, M. Panos, (Eds.), Handbook of global optimization, Kluwer Academic Publishers (1995).

[82] P. Shen, K. Zhang, Y. Wang, Applications of interval arithmetic in non-smooth global optimization, Appl. Math. Comput. 144 (2003) 413–431.

[83] C.Y. Gau, M.A. Stadtherr, Reliable nonlinear parameter estimation using interval analysis: error-in-variable approach, Comput. Chem. Eng. 24 (2000) 631–637.

[84] W.R. Esposito, C.A. Floudas, Parameter estimation in nonlinear algebraic models via global optimization, Comput. Chem. Eng. 22 (1998) S213–S220.

[85] W.R. Esposito, C.A. Floudas, Global optimization for the parameter estimation of differential-algebraic systems, Indust. Eng. Chem. Res. 39 (2000) 1291–1310.

[86] W.R. Esposito, C.A. Floudas, Deterministic global optimization in nonlinear optimal control problems, J. Global Opt. 17 (2000) 97–126.

[87] C.S. Adjiman, S. Dallwing, C.A. Floudas, A. Neumaier, A global optimization method, αBB, for general twice-differentiable constrained NLPs-I. Theoretical advances, Comp. Chem. Eng. 22 (1998) 1159–1179.

[88] C.S. Adjiman, I.P. Androulakis, C.A. Floudas, A global optimization method, αBB, for general twice-differentiable constrained NLPs-II. Implementation and computational results, Comput. Chem. Eng. 22 (1998) 1159–1179.

[89] I. Papamichail, C.S. Adjiman, A rigorous global optimization algorithm for problems with ordinary differential equations, J. Global Optim. 24 (2002) 1–33.

[90] I. Papamichail, C.S. Adjiman, Global optimization of dynamic systems, Comput. Chem. Eng. 28 (2004) 403–415.

[91] A.B. Singer, J.K. Bok, P.I. Barton, Convex underestimators for variational and optimal control problems, Comp. Aided Chem. Eng. 9 (2001) 776–772.

[92] C.A. Floudas, Recent advances in global optimization for process synthesis, design and control: enclosure of all solutions, Comput. Chem. Eng. (1999) S963–973.

[93] N.V. Sahinidis, M. Tawarmalani, Applications of global optimization to process and molecular design, Comput. Chem. Eng. 24 (2000) 2157–2169.

[94] W.R. Esposito, C.A. Floudas, Deterministic global optimization in isothermal reactor network synthesis, J. Global Optim. 22 (2002) 59–95.

[95] S. Brooks, A discussion of random methods for seeking maxima, Oper. Res. 6 (1958) 244–251.

[96] L.A. Rastrigin, Y. Rubinstein, The comparison of random search and stochastic approximation while solving the problem of optimization, Autom. Contr. 2 (1969) 23–29.

[97] W.L. Price, Global optimization by controlled random search, J. Optimiz. Theory App. 40 (1983) 333–348.

[98] J.R. Banga, J.J. Casares, ICRS: application to a wastewater treatment plant model. In “Process Optimisation”, IChemE Symposium Series No. 100, Pergamon Press (1987) 183–192.

[99] A.A. Törn, Global optimization as a combination of global and local search, Proceedings of Computer Simulation versus Analytical Solutions for Business and Economic Models (1973) 191–206.

[100] A.H.G. Rinnooy-Kan, G.T. Timmer, Stochastic global optimization methods. Part I: clustering methods, Math. Program. 39 (1987) 27–56.

[101] D.B. Fogel, Evolutionary computation: toward a new philosophy of machine intelligence, IEEE Press (2000).

[102] S. Kirkpatrick, C.D. Gellatt, M.P. Vecchi, Optimization by simulated annealing, Science 220 (1983) 671–680.

[103] F. Glover, M. Laguna, Tabu Search, Kluwer Academic Publishers (1997).

[104] C. Wang, H. Quan, X. Xu, Optimal design of multiproduct batch chemical processes using tabu search, Comput. Chem. Eng. 23 (1999) 427–437.

[105] M. Dorigo, G. Caro, The ant colony optimization meta-heuristic, In D. Corne, M. Dorigo, F. Glover, (Eds.), New ideas in optimization, McGraw–Hill (1989).

[106] M. Mathur, S.B. Karale, S. Prive, V.K. Jayaraman, B.D. Kulkarni, Ant colony approach to continuous function optimization, Ind. Eng. Chem. Res. 39 (2000) 3814–3822.

[107] J.H. Holland, Adaptation in natural and artificial systems, University of Michigan Press (1975).

[108] J.H. Holland, Adaptation in natural and artificial systems, The MIT Press. Cambridge (1992).

[109] Z. Michalewicz, D. Dasgupta, R.L. Riche, M. Schoenauer, Evolutionary algorithms for constrained engineering problems, Comput. Ind. Eng. Journal 30 (1996) 851–870.

[110] L.J. Fogel, A.J. Owens, M.J. Walsh, Artificial intelligence through simulated evolution, John Wiley & Sons (1996).

[111] I. Rechenberg, Evolutionsstrategie: optimierung technisher systeme nach principien der biologischen evolution, Frommann–Holzboog (1973).

[112] H.P. Schwefel, Evolution and optimum seeking, Wiley (1995).

[113] T.P. Runarsson, X. Yao, Stochastic ranking for constrained evolutionary optimization, IEEE Trans. Evol. Comput. 4 (2000) 284–294.

[114] T.R. Bhat, D. Venkataramani, V. Ravi, C.V.S. Murty, An improved differential evolution method for efficient parameter estimation in biofilter modelling, Biochem. Eng. J. 28 (2006) 167–176.

[115] J.E. Jiménez-Hornero, I. Santos-Dueñas, I. García-García, Structural identifiability of a model for the acetic acid fermentation process. Math. Biosci. 216 (2008) 154-162.

[116] I. García-García, D. Cantero-Moreno, C. Jiménez-Ot, S. Baena-Ruano, J.E. Jiménez-Hornero, I. Santos-Dueñas, J. Bonilla-Venceslada, F. Barja, Estimating the mean acetification rate via on-line monitored changes in ethanol during a semi-continuous vinegar production cycle, J. Food Eng. 80 (2007) 460–464.

[117] F.J. Nieto, Algunos aspectos de la tecnología de la fermentación acética, In C. Llaguno, M.C. Polo (Eds.), El vinagre de vino, CSIC (1991).

[118] A.R. Conn, N.I.M. Gould, P.L. Toint, A globally convergent augmented lagrangian algorithm for optimization with general constraints and simple bounds, SIAM J. Numer. Anal. 28 (1991) 545–572.

[119] A.R. Conn, N.I.M. Gould, P.L. Toint, A globally convergent augmented lagrangian barrier algorithm for optimization with general inequality constraints and simple bounds, Math. Comput. 66 (1997) 261–288.

[120] www.ecosimpro.com

[121] S. Baena-Ruano, C. Jiménez-Ot, I. Santos-Dueñas, D. Cantero-Moreno, F. Barja, I. García-García, Rapid method for total, viable and non-viable acetic acid bacteria determination during acetification process, Process Biochem. 41 (2006) 1160–1164.

[122] A.M. Law, W.D. Kelton, Simulation modeling and analysis, McGraw–Hill (2000).

[123] I. García-García, I.M. Santos-Dueñas, C. Jiménez-Ot, J. E. Jiménez-Hornero, J.L. Bonilla-Venceslada. Vinegar Engineering. In P. Giudici, L. Solieri (Eds), Vinegars of the World, Chapter 6. Springer (2008).

Figure captions

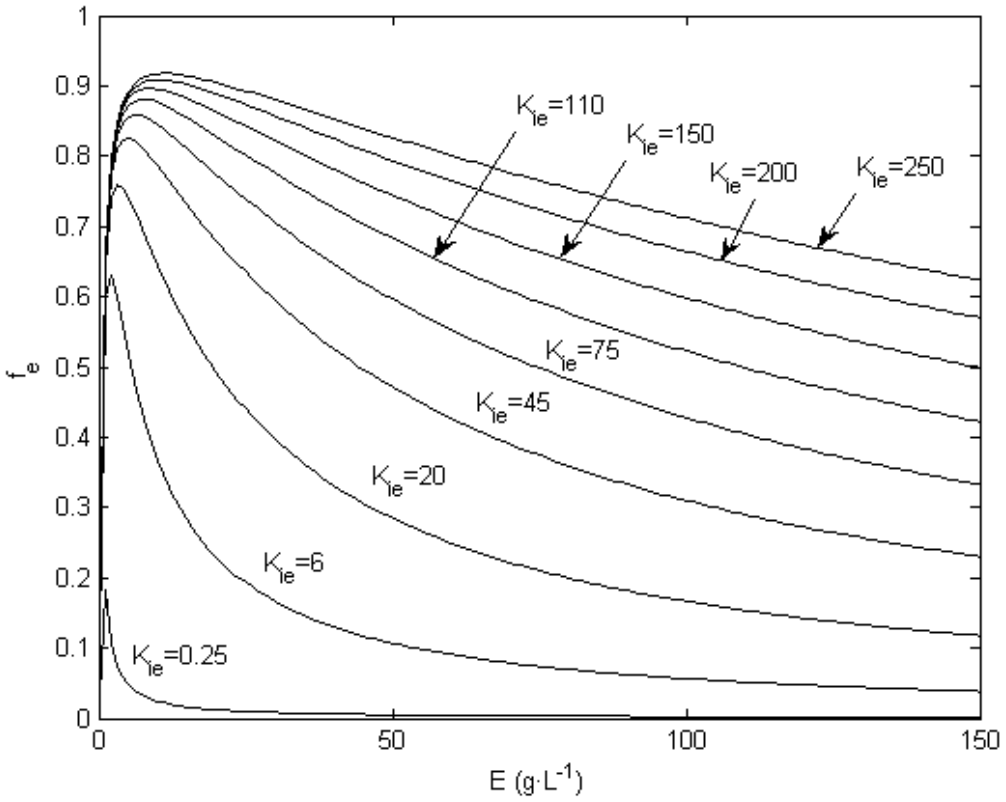

Figure 1: Variation of f_e with ethanol concentration (E) at different K_{IE} values using K_{SE} = 0.5.

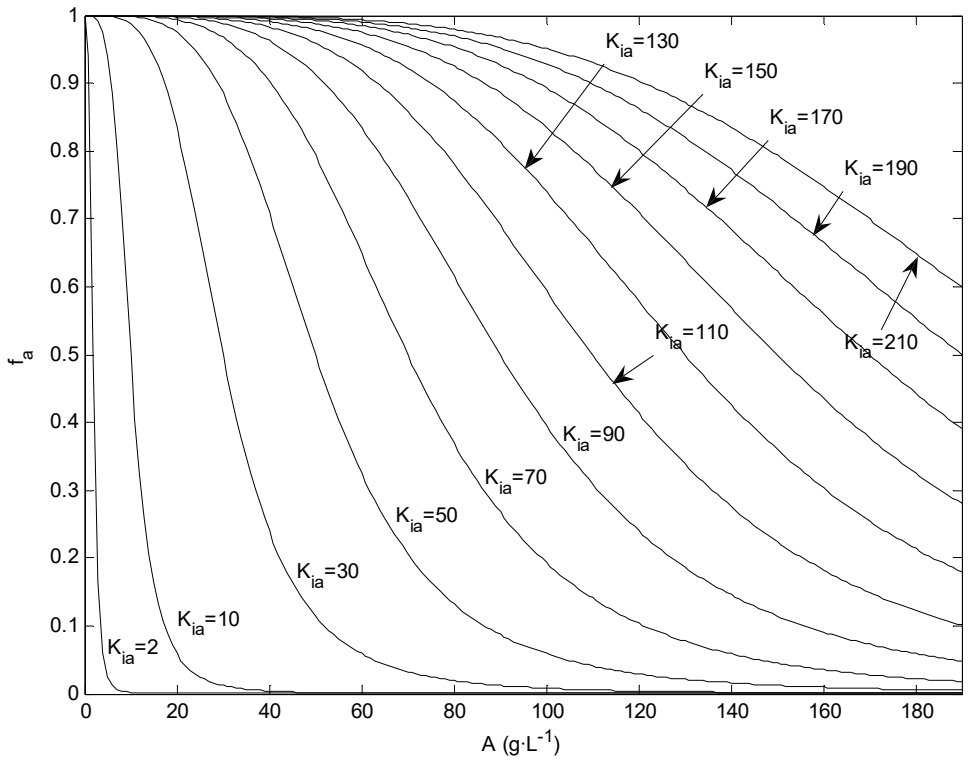

Figure 2: Variation of f_a with acetic acid concentration (A) at different K_{IA} values.

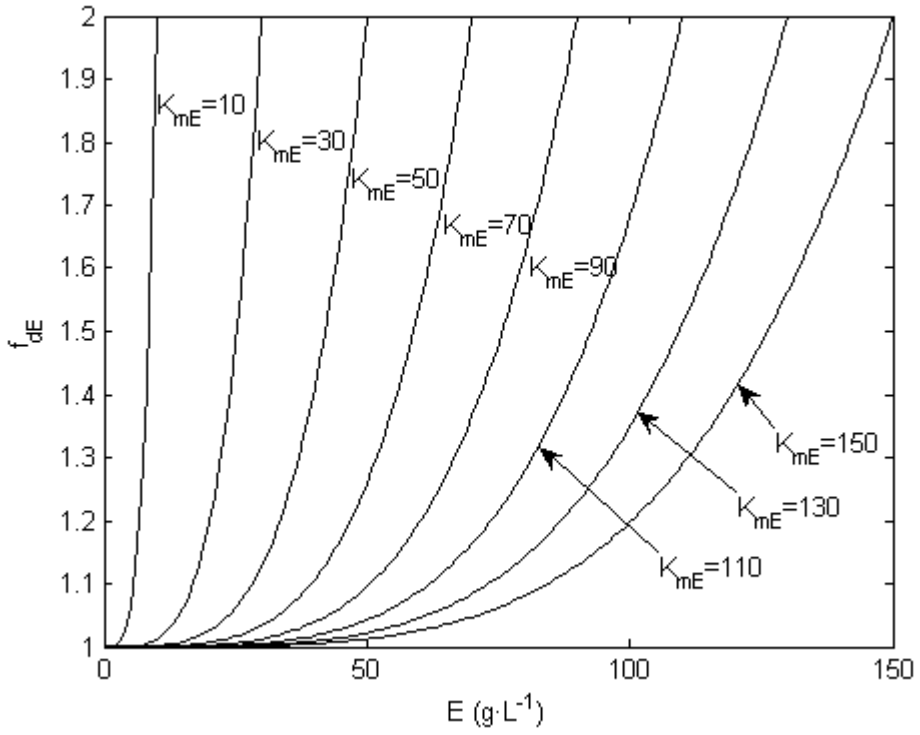

Figure 3: Variation of f_{dE} with the ethanol concentration (E) at different K_{mE} values.

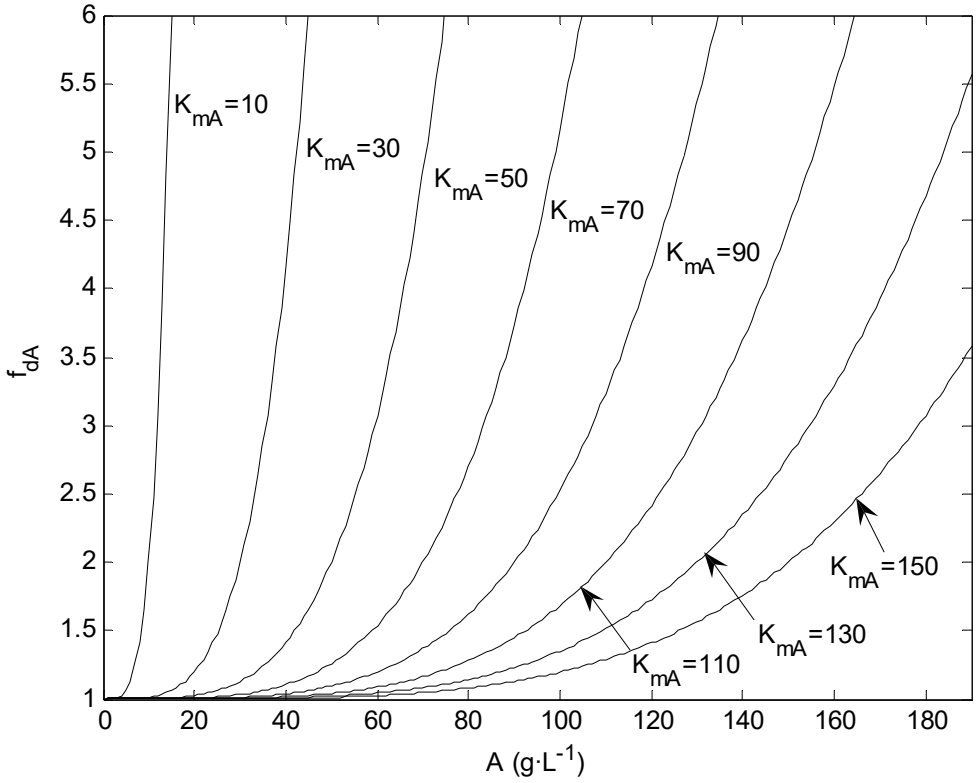

Figure 4: Variation of f_{dA} with the acetic acid concentration (A) at different K_{mA} values.

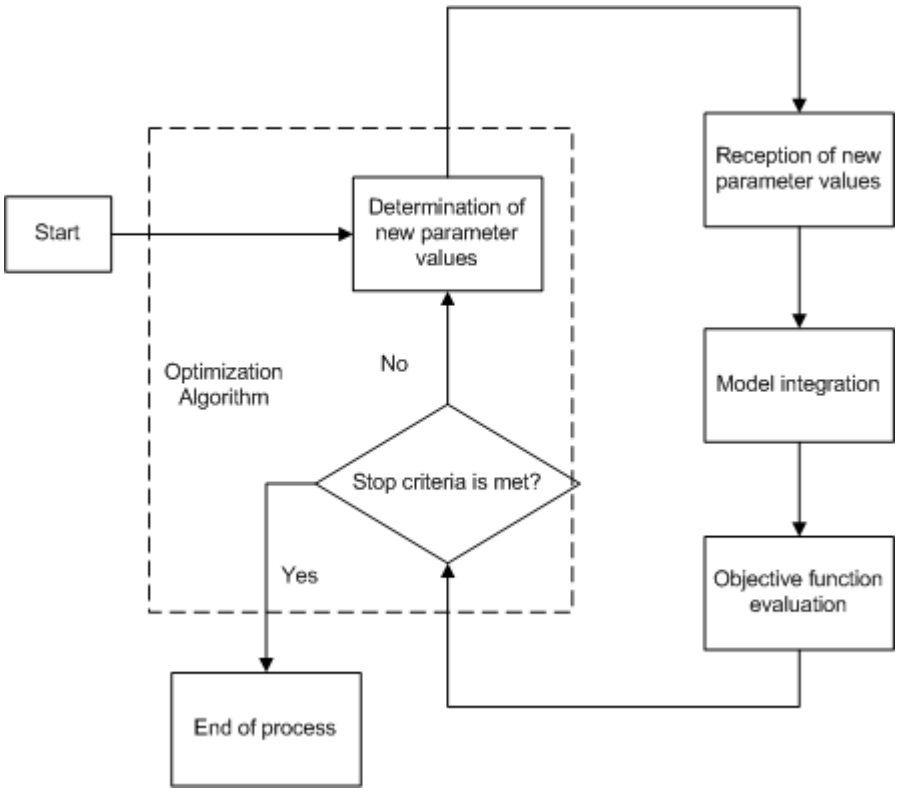

Figure 5: Flow-chart of the optimization procedure.

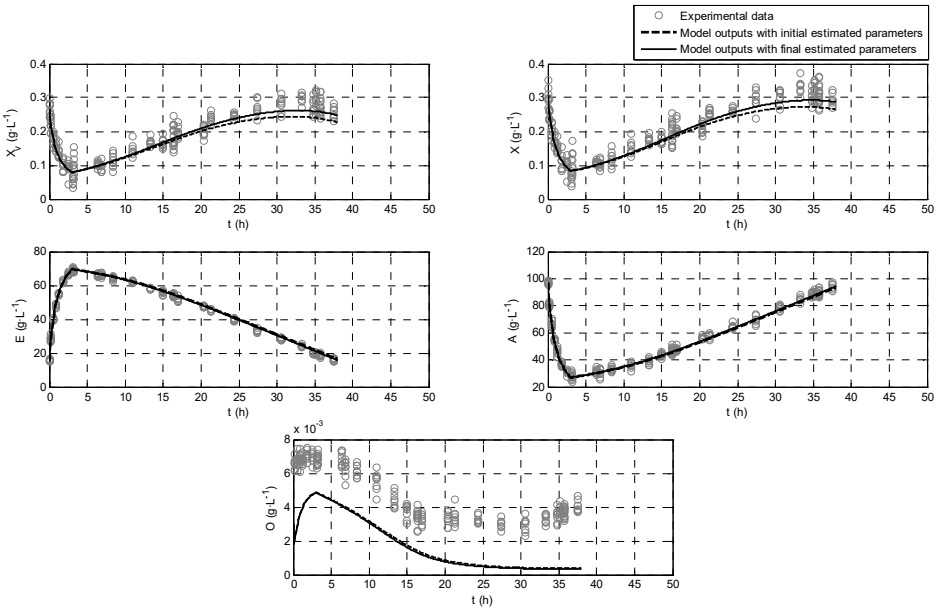

Figure 6: Comparison of the model outputs obtained by using the initial and optimal parameter sets with experimental data from test A1 following execution of ALGA.

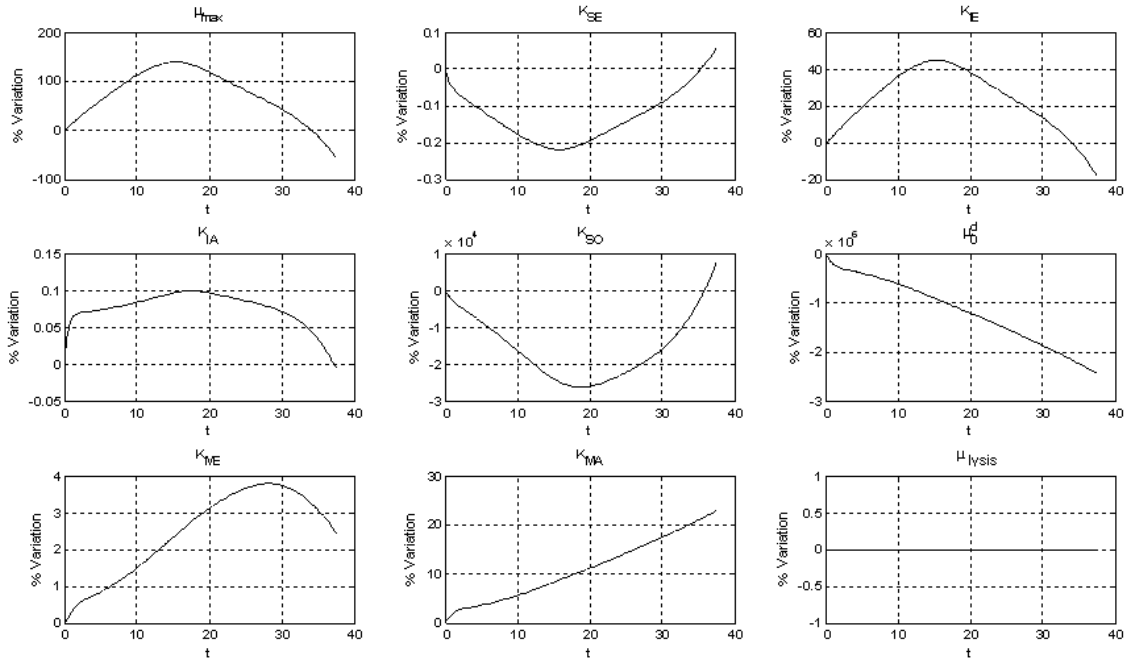

Figure 7: Percent variations of the sensitivity functions with respect to the concentration of viable cells (X_v) as a function of time (t, h) in test A1.

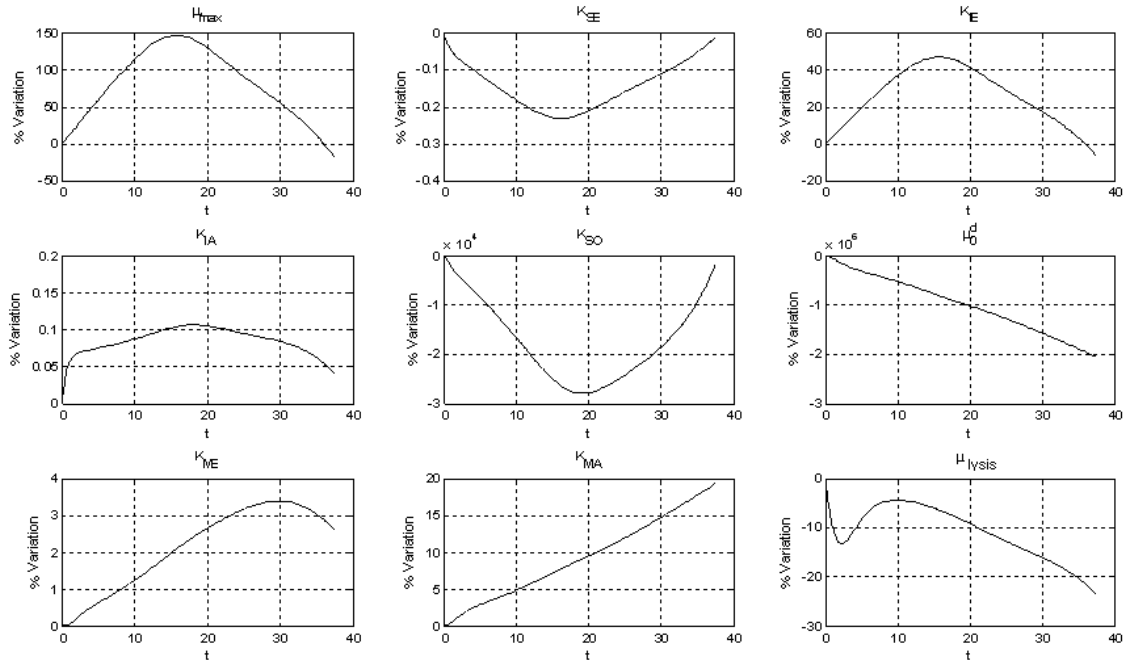

Figure 8: Percent variations of the sensitivity functions with respect to the concentration of total cells (X) as a function of time (t, h) in test A1.

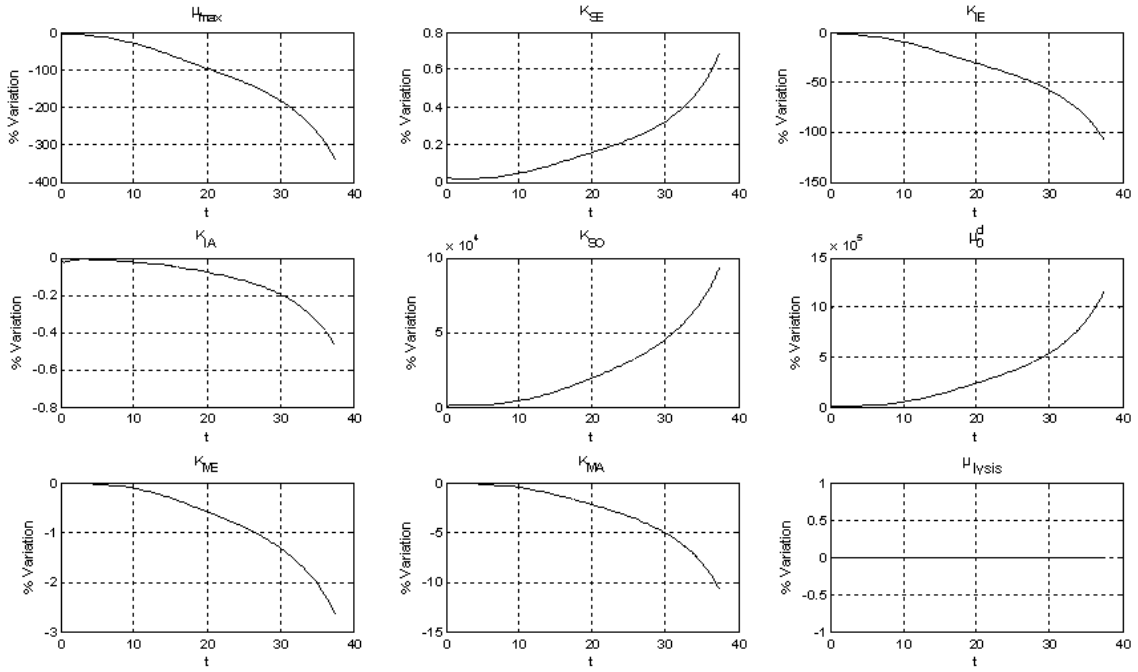

Figure 9: Percent variations of the sensitivity functions with respect to the concentration of ethanol (E) as a function of time (t, h) in test A1.

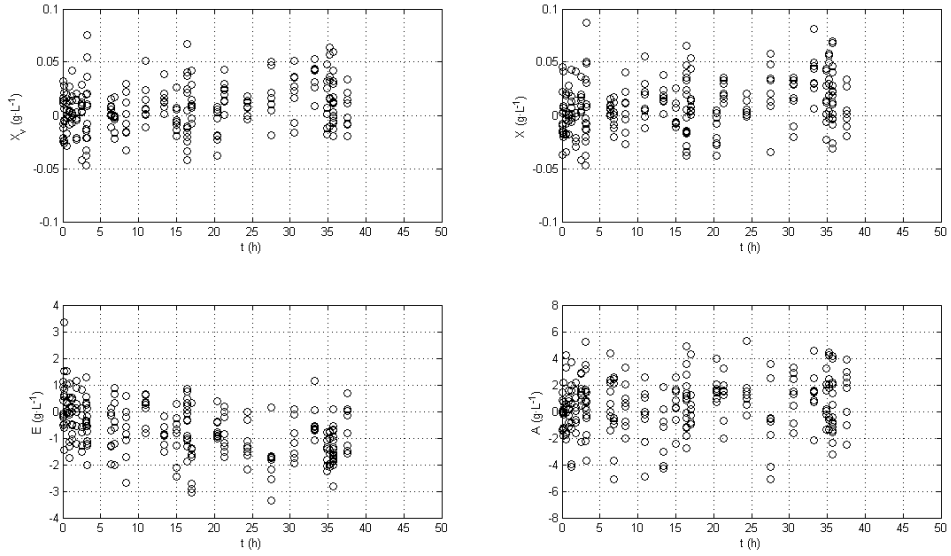

Figure 10: Residuals obtained with the optimal parameter set for test A1.

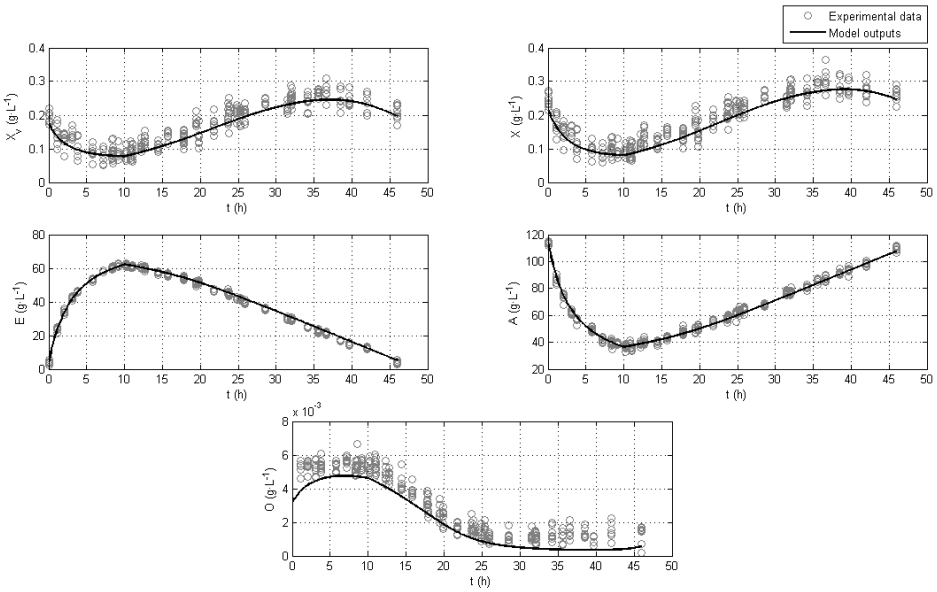

Figure 11: Comparison of the model outputs obtained by using the optimal parameter set with experimental data from test C1.

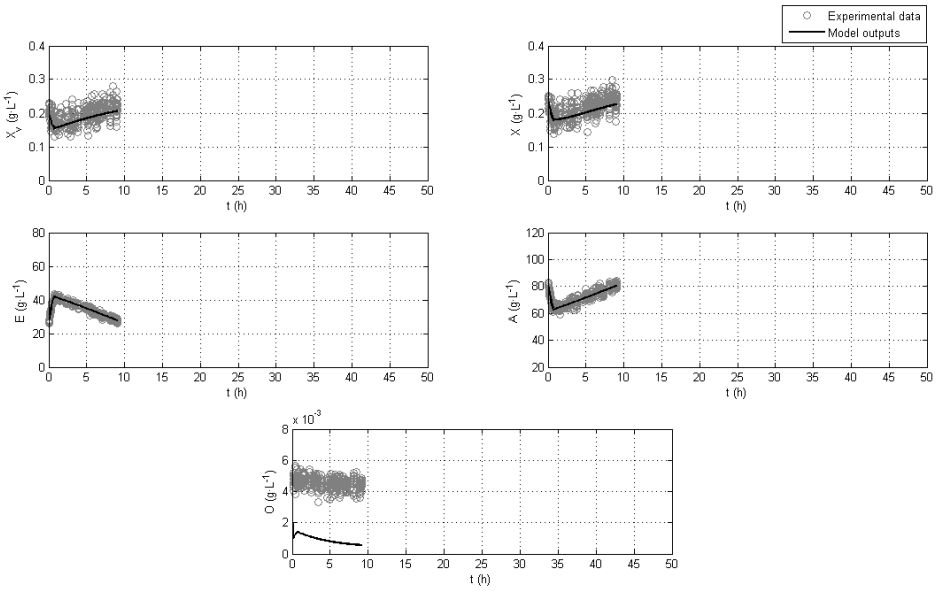

Figure 12: Comparison of model outputs obtained by using the optimal parameter set with experimental data for test C2.

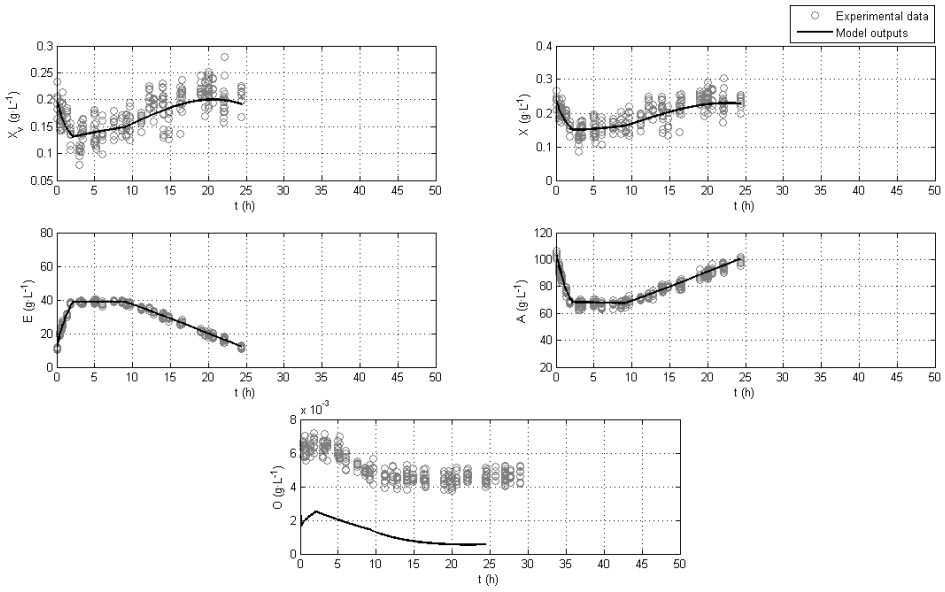

Figure 13: Comparison of model outputs obtained by using the optimal parameter set with experimental data for test C3.

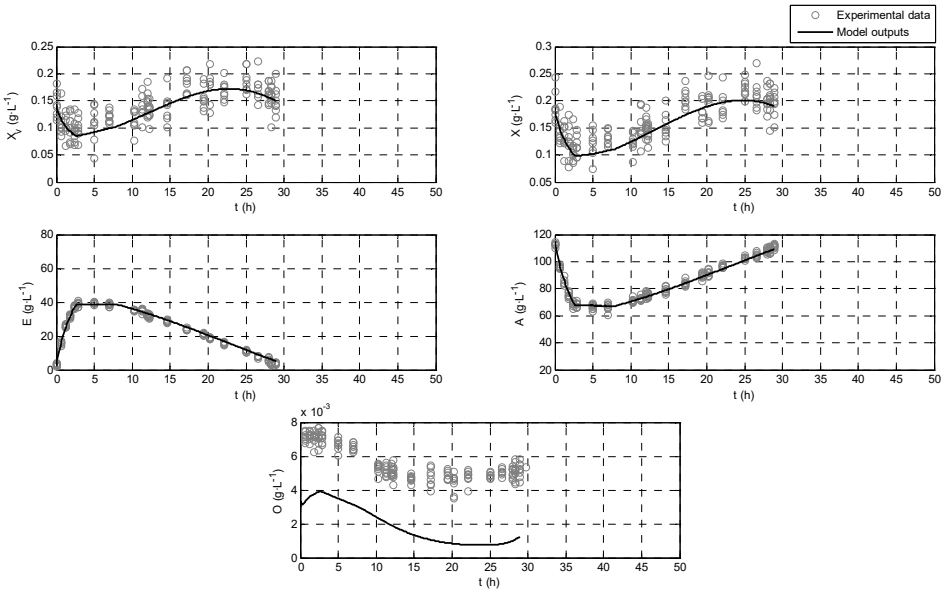

Figure 14: Comparison of model outputs obtained by using the optimal parameter set with experimental data for test C4.